Journal of Geosciences, 56 (2011), 343–357 DOI: 10.3190/jgeosci.109

Original paper

Emplacement, structural and P–T evolution of the ~346 Ma Miřetín Pluton (eastern Teplá–Barrandian Zone, Bohemian Massif): implications for regional transpressional tectonics

Lukáš VONDROVIC[1,2]*, Kryštof VERNER[1,2], David BURIÁNEK[3], Patricie HALODOVÁ[4], Václav KACHLÍK[5], Jitka MÍKOVÁ[4]

[1] *Czech Geological Survey, Klárov 3, 118 21 Prague 1, Czech Republic; lukas.vondrovic@geology.cz*
[2] *Institute of Petrology and Structural Geology, Charles University, Albertov 6, 128 43 Prague 2, Czech Republic*
[3] *Czech Geological Survey, Leitnerova 22, 658 69 Brno, Czech Republic*
[4] *Czech Geological Survey, Geologická 6, 152 00 Prague 5, Czech Republic*
[5] *Institute of Geology and Palaeontology, Charles University, Albertov 6, 128 43 Prague 2, Czech Republic*
* *Corresponding author*

The calc-alkaline Miřetín Pluton (newly dated at 346 Ma ± 5 Ma; an U–Pb age obtained by laser-ablation ICP MS method on zircons) is a NNE–SSW elongated intrusive body emplaced into the upper- to mid- crustal rocks of the Polička Unit (eastern Teplá–Barrandian Zone; Bohemian Massif). Its composition reveals similarities to other calc-alkaline granitoids, which are mostly interpreted as products of magma mixing between the basic magmas derived from mantle wedge above a subduction zone with crustally-derived acid melts. The conditions of magma crystallization estimated at 653–681 °C and 0.29–0.43 GPa roughly correspond to peak metamorphic evolution of the host volcano-sedimentary rocks of the northwestern part of the Polička and Hlinsko units. The Miřetín Pluton was emplaced into a NNE–SSW oriented transpressional domain, well recognized on a regional scale along the eastern margin of the Teplá–Barrandian Zone. During, or shortly after the magma emplacement, the Miřetín Pluton was affected by pervasive submagmatic to high-T solid-state deformation, reflecting an additional strain increment of regional transpression in a narrow zone of thermal softening. Sharply superimposed low-T solid-state fabric preserved along the western part of the Pluton was connected with normal shearing between the Polička Unit at the bottom and the overlying Hlinsko Unit after 335 Ma.

Keywords: European Variscides, Bohemian Massif, Miřetín Pluton, emplacement, transpression, U–Pb zircon dating
Received: 27 April 2011; accepted: 17 December 2011; handling editor: J Žák

1. Introduction

Fabrics in granitoid intrusions commonly reflect magma emplacement and/or a record of regional geodynamic processes (e.g. changes in the regional strain field, regional kinematic framework and local exhumation paths), which could have operated during and/or after the magma crystallization (e.g. Paterson et al. 1998). The structural framework of granitoids emplaced during transpression reflects an interplay between local strain field and regional deformation of host rocks, thermo-mechanical effects of the crystallized magma and development of transitional magmatic to subsolidus fabrics (e.g. Tikoff and Greene 1997; Saint Blanquat et al. 1998; Chardon et al. 1999; Brown and Solar 1999; Miller and Paterson 2001; Schmidt and Paterson 2002). Many analogous studies revealing relationships between magmatic and tectonic processes were also recently performed in the Bohemian Massif (e.g. Schulmann et al. 2005; Žák et al. 2005, 2011; Verner et al. 2008, 2009).

This work focuses on reconstruction of a regional geodynamic event which occurred during and shortly after the crystallization of the ~346 Ma Miřetín Pluton, emplaced into the mid- to upper-crustal levels of units at the NE periphery of the Moldanubian Zone (Fig. 1a–b). On a regional scale, it took place before the high-grade metamorphism and exhumation of the deep-seated rocks of the Moldanubian Zone located to the S (e.g. Vrána et al. 1995; Schulmann et al. 2008). The genesis of similar plutons of calc-alkaline composition (e.g. ~354 Ma Sázava Pluton of the Central Bohemian Plutonic Complex; Janoušek et al. 2004, 353–346 Ma Zábřeh Intrusive Complex, Budislav and Miřetín plutons; Verner et al. 2009; Vondrovic and Verner 2010) has been interpreted as one of magmatic-arc granites (e.g. Finger et al. 1997; Schulmann et al. 2009; Žák et al. 2011). In a broad sense, most of these intrusions were emplaced in relation to the regional Late Devonian to Early Carboniferous (356–346 Ma) transpressional or compressional tectonic event, which took place along the eastern margin of the upper-crustal Teplá–Barrandian Zone (Žák et al. 2005, 2011; Verner et al. 2009; Pertoldová et al. 2010).

Based on combination of field structural data, microstructural and EBSD analyses, U–Pb zircon dating and

estimation of P–T conditions of magma crystallization we provide new insights into emplacement mechanisms and subsequent geodynamic evolution of the Miřetín Pluton and its surrounding units of the easternmost flank of the Teplá–Barrandian Zone.

2. Regional geological setting

In a broad sense, the studied area (the Miřetín Pluton and its host upper- to mid-crustal Polička and Hlinsko units; Fig. 1a–c) is assumed to belong to the eastern extension of the Teplá–Barrandian Zone (e.g. Mísař et al. 1983; Verner et al. 2009; Pertoldová et al. 2010). However, some authors also pointed out its lithological affinities to the Western Sudetes (e.g. Cháb et al. 2010). The Teplá–Barrandian Zone crops out between the high-grade Moldanubian Zone in the southeast and the Saxothuringian Zone in the west to north. The central part of the Teplá–Barrandian Zone contains Neoproterozoic to Lower Palaeozoic unmetamorphosed volcanic and sedimentary rocks, which did not undergo strong Variscan metamorphism. In contrast, its margins (e.g. Teplá, Domažlice, Železné Hory, Hlinsko and Polička units) were exposed to an amphibolite-facies Variscan overprint (Cháb et al. 1995). The southern and eastern

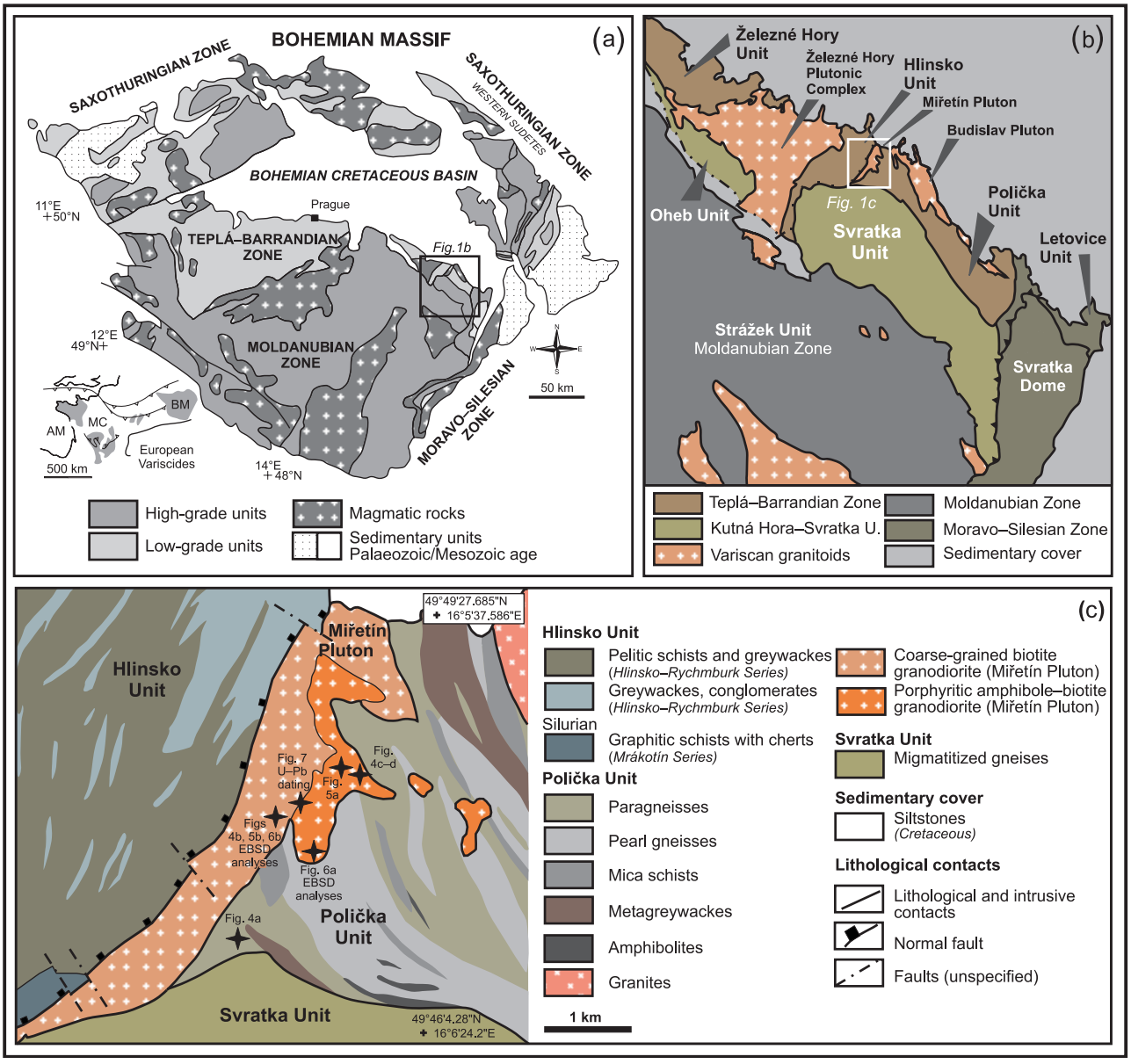

Fig. 1a – Schematic map of the Bohemian Massif, modified after Franke (2000); **b** – Schematic sketch of the NE part of the Bohemian Massif (NE periphery of the Moldanubian Zone); **c** – Geological outline of the studied area (Miřetín Pluton and its host rocks of the Polička and Hlinsko units) based on geological map 1:50 000, sheet 14-33 Polička (Stárková ed. 1998). Locations of studied samples and photographs are also shown.

Teplá–Barrandian Zone was intruded by numerous granitoid bodies of calc-alkaline composition (Holub et al. 1997a, b; Hrouda et al. 1999; Janoušek et al. 2000; Žák et al. 2005, 2011; Verner et al. 2009).

The *Hlinsko Unit* (Fig. 1b–c) is bound by the Železné hory Plutonic Complex in the W, mid-crustal Svratka Unit in the S and upper- to mid-crustal Polička Unit in the E. Eastern part of the Hlinsko Unit is separated from the Polička Unit by a NNE–SSW trending normal shear zone (e.g. Pitra et al. 1994). The Hlinsko Unit is composed of two different metasedimentary formations folded into a large, NNE–SSW elongated synform: (i) the prevailing Hlinsko–Rychmburk Formation composed of greywackes and metapelites with minor layers of metavolcanic rocks (e.g. Vachtl 1962) and (ii) the Mrákotín Formation built by dark phyllitic slates to graphitic schists and phyllites with quartzite intercalations, forming the central part of the Hlinsko synform (e.g. Štorch and Kraft 2009). The age of the Hlinsko–Rychmburk Formation is unknown; however it is assumed to be Neoproterozoic to Early Carboniferous (Pitra et al. 1994 and references therein). The Mrákotín Formation was assigned to the Silurian based on paleontological data (Würm 1927; Štorch and Kraft 2009). The Variscan regional metamorphism in the Hlinsko Unit metapelites attained peak pressures of 0.35–0.40 GPa and temperatures of 530–570 °C (Pitra and Guiraud 1996).

The Hlinsko Unit recorded a polyphase Variscan geodynamic evolution. The oldest metamorphic structures are cleavage planes related to non-cylindrical recumbent folding of the primary bedding. These cleavages are accompanied by a subhorizontal ~NW–SE mineral lineation (Pitra et al. 1994). The superimposed deformation stage was connected with ~E–W shortening, which produced various types of folds with W or E moderately to steeply dipping axial planes and also the large-scale synform of the whole Hlinsko Unit. This compressional event was connected with a subsequent generation of ~N–S (NNE–SSW) axial cleavages (Pitra et al. 1994).

The *Polička Unit* is composed of metamorphosed volcano-sedimentary sequences of unknown age (Buriánek et al. 2003; Buriánek and Pertoldová 2009; Verner et al. 2009). Its northern part is lithologically monotonous, composed of rhythmically alternating metagreywackes and schists with scarce intercalations of metaconglomerates, fine-grained amphibolites, calc-silicate rocks and marbles. During Variscan orogeny, regional tectonometamorphic processes under greenschist- to amphibolite-facies conditions affected these rocks. Degree of regional metamorphism gently increases towards the E to SE. For the northwestern Polička Unit the P–T conditions were estimated at 559 ± 65 °C and 0.3 ± 0.2 GPa, for the central and eastern parts at 564–640 °C and 0.49–0.64 GPa (Buriánek 2009; Pertoldová et al. 2010).

The overall structural pattern is defined by pervasive schistosity dipping in the central and eastern parts under moderate angles to the ~NE or ~SW. The regional metamorphic fabrics along the western flank of this unit dip under moderate angles to ~WNW or NE. Across the whole Polička Unit, the regional fabrics bear a gently to moderately ~WNW-plunging stretching or mineral lineation and indicators of right-lateral or thrusting kinematics (Verner et al. 2009).

Metamorphic rocks of the Polička Unit were intruded by several granitoid bodies, mainly of calc-alkaline composition (e.g. Miřetín and Budislav plutons). The Miřetín Pluton was emplaced into the northwestern part of the Polička Unit (Fig. 1c) and its intrusive contacts are mostly parallel to the regional metamorphic structures. Original contacts with the Hlinsko Unit in the W were later modified by large-scale normal faults (Fig. 1c). The Pluton has an irregular NNE–SSW elongated outline with approximate dimensions of ~8 km (NNE–SSW) and ~1.5 km (WNW–ESE). Granitoids of the Miřetín Pluton (SiO_2 = 59.3–65.0 wt. %) are high-K calc-alkaline (K_2O = 2.4–4.0 wt. %) and subaluminous (A/CNK = 0.9–1.2); the trace-element signature clearly indicates their magmatic-arc origin (e.g. Buriánek et al. 2003).The rocks of Miřetín Pluton (biotite and amphibole–biotite granodiorites) were affected by pervasive deformation and limited recrystallization at relatively high temperatures.

3. Analytical techniques

Note that the brief description and GPS coordinates of samples studied by individual methods is given in Tab. 1 and shown on Fig. 1c.

Tab. 1 List and location of studied samples

Sample	Locality	Analyses	Rock type	Loc. type	X-coordinate*	Y-coordinate*
404	Pastvisko	petrology	tonalite	outcrop	49°47'23.977"	16°5'52.805"
L23	Kutřín	petrology	medium-grained Amp–Bt granodiorite	outcrop	49°49'8.846"	16°3'41.955"
LV13S	Kutřín	petrology	porphyritic Amp–Bt granodiorite	outcrop	49°49'21.380"	16°3'34.622"
L136	Rychnov	EBSD	porphyritic Amp–Bt granodiorite	quarry	49°46'59.270"	16°4'12.429"
L90	Otradov	EBSD	coarse-grained Bt granodiorite	outcrop	49°47'38.193"	16°3'15.751"
LV92	Otradov	U–Pb dating	porphyritic Amp–Bt granodiorite	outcrop	49°47'34.546"	16°3'25.188"

*WGS-84 = World Geodetic System 1984

3.1. Mineral chemistry

Chemical analyses of the minerals were obtained using a Cameca SX-100 electron microprobe at the Joint Electron Microprobe Laboratory of the Masaryk University and the Czech Geological Survey in the Brno village. The measurements were carried out in a wave dispersion mode using 15 kV of acceleration voltage, 5 µm of beam diameter, 30 nA of current and integration time of 20 s. The crystallochemical formulae of feldspar were recalculated to 8 and those of micas to 22 oxygen atoms. The amphibole formulae were obtained assuming 23 O, 2 (OH, F, Cl) and Fe^{3+}/Fe^{2+} ratios were estimated based on 13 cations except Ca, Na and K (Leake et al. 1997). The mineral abbreviations are according to Kretz (1983).

The solidus temperatures of the Miřetín Pluton were estimated using the thermometer of Holland and Blundy (1994) from amphibole and plagioclase rim compositions. These thermometers perform well (± 40 °C) in the range 400–1000 °C and 0.1–1.5 GPa over a broad range of bulk compositions. The usable mineral compositions are restricted to amphiboles with $Na^A > 0.02$ pfu, $^{VI}Al >$ 1.8 pfu, and Si of 7.0–6.0 pfu and plagioclases with X_{an} of 0.1–0.9. The Al-in-hornblende barometer of Anderson and Smith (1995) is recommended for amphiboles with $Fe/(Mg + Fe) \leq 0.65$.

3.2. Electron back-scatter diffraction (EBSD)

The lattice preferred orientation (LPO) of quartz aggregates was measured using the EBSD method (see Prior et al. 1999 for overview of its principles) on a CamScan 3200 scanning electron microscope at the Czech Geological Survey, Prague. The EBSD patterns were recorded using a HKL Technology Nordlys II camera system and indexed using the Channel5 software (Schmidt and Olensen 1989). Pattern acquisition was carried out using acceleration voltage of 20 kV, beam current of ~5 nA, working distance of 33 mm and sample tilt of 70°. The analyses were performed in the manual mode; each individual grain is represented by one orientation measurement. Crystallographic orientation data given by three Euler angles φ_1, Φ, φ_2 were obtained from interactively indexed EBSD patterns. We used the crystallographic parameters of Bonlen et al. (1980) for quartz indexation. The LPO patterns of quartz are presented in stereonets, lower hemisphere equal area projection.

3.3. U–Pb dating

A Thermo-Finnigan Element 2 sector field ICP-MS coupled to a 213 Nd:YAG laser (New Wave Research UP-213) at Bergen University, Norway was used to measure the Pb/U and Pb isotopic ratios in zircons. Laser-ablation ICP-MS isotopic analysis of zircons followed the technique described in Košler et al. (2002) and Košler and Sylvester (2003). The sample introduction system enabled

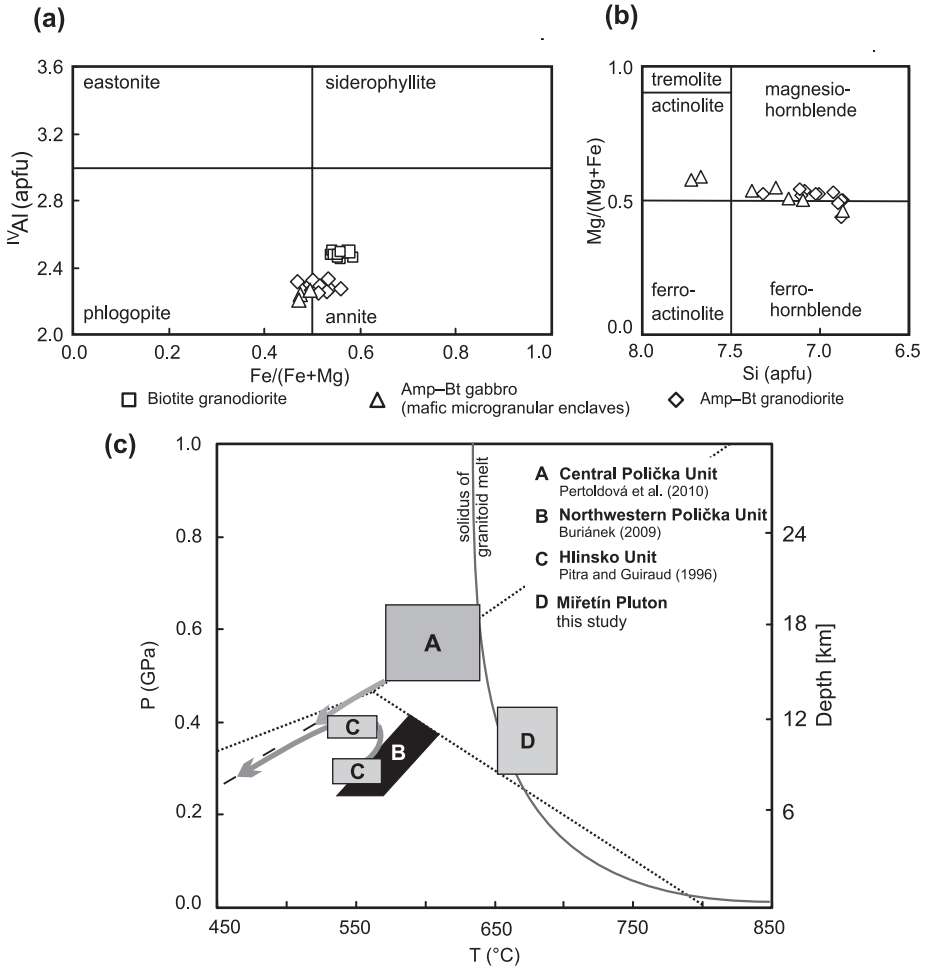

Fig. 2a Fe/(Fe + Mg) vs. ^{IV}Al classification diagram for biotites (Miřetín Pluton); **b** – Mg/(Fe + Mg) vs. Si (apfu) classification diagram for amphiboles (after Leake et al. 1997) **c** – Summary P–T diagram showing inferred paths of regional metamorphic evolution for the Polička and Hlinsko units (taken from literature) as well as crystallization conditions of the Miřetín Pluton (this study).

Tab. 2 Representative compositions of feldspars (wt. % and apfu)

Sample	L23	L23	L23	404	404	404	LV13S	LV13S	LV13S
SiO_2	59.20	59.31	57.35	58.55	57.68	59.35	61.74	61.51	65.17
P_2O_5	0.00	0.02	0.00	0.04	0.00	0.00	0.10	0.09	0.00
Al_2O_3	25.93	25.77	26.80	26.05	26.31	25.77	23.93	24.16	18.10
FeO	0.05	0.06	0.04	0.01	0.02	0.33	0.01	0.03	0.01
CaO	7.61	7.81	9.06	8.13	8.80	7.95	5.83	5.92	0.00
Na_2O	7.15	7.00	6.33	6.77	6.58	7.09	8.18	8.20	0.23
K_2O	0.23	0.21	0.22	0.26	0.15	0.20	0.29	0.21	16.22
BaO	0.00	0.00	0.02	0.00	0.00	0.00	0.00	0.02	0.07
SrO	0.08	0.13	0.08	0.11	0.11	0.09	0.04	0.08	0.09
Total	100.18	100.18	99.80	99.81	99.54	100.69	100.08	100.12	99.74
(apfu)									
Si	2.638	2.642	2.576	2.622	2.596	2.632	2.739	2.728	3.013
Al	1.362	1.353	1.419	1.375	1.395	1.347	1.251	1.263	0.987
Fe^{3+}	0.002	0.002	0.001	0.001	0.001	0.012	0.000	0.001	0.001
T-site	4.002	3.997	3.997	3.997	3.992	3.991	3.991	3.992	4.000
K	0.013	0.012	0.013	0.015	0.009	0.011	0.016	0.012	0.957
Na	0.618	0.605	0.552	0.588	0.574	0.609	0.703	0.705	0.020
Ca	0.359	0.368	0.431	0.385	0.419	0.373	0.274	0.278	0.000
Ba	0.000	0.000	0.000	0.000	0.000	0.000	0.000	0.000	0.001
Sr	0.002	0.003	0.002	0.003	0.003	0.002	0.001	0.002	0.002
O-site	0.992	0.988	0.997	0.991	1.005	0.996	0.994	0.997	0.981
Mol %									
An	36.2	37.4	43.3	39.0	41.8	37.5	27.6	27.9	0.0
Ab	62.4	61.4	55.5	59.5	57.3	61.3	70.8	70.9	2.1
Or	1.3	1.2	1.3	1.5	0.9	1.1	1.6	1.2	97.9

simultaneous nebulisation of a tracer solution and laser ablation of the solid sample (Horn et al. 2000). Tracer solution containing natural Tl ($^{205}Tl/^{203}Tl$ = 2.3871; Dunstan et al. 1980), ^{209}Bi and enriched ^{233}U and ^{237}Np (> 99 %) was aspirated through an Apex desolvation nebuliser (Elemental Scientific) and mixed with the sample from the laser cell, resulting in a mixture of sample and tracer solution dry aerosol, which entered the plasma. The laser was set up to produce an energy density of *c*. 5 J/cm^2 at a repetition rate of 10 Hz. The sample was placed in the ablation cell, which was moved during ablation at a speed of 10 μm·s^{-1} beneath the stationary laser beam to produce a linear grid (*c*. 20 × 100 μm) in the sample. Typical sequence consisted of a 40 s measurement of analytes in the gas blank and aspirated tracer solution, followed by acquisition of the U and Pb signals from zircon, along with the continuous signal from the aspirated tracer solution, for another 160 s. The data were acquired in the time-resolved – peak jumping – pulse counting mode with 1 point measured per peak for masses 202 (flyback), 203 and 205 (Tl), 206 and 207 (Pb), 209 (Bi), 233 (U), 237 (Np), 238 (U), 249 (^{233}U oxide), 253 (^{237}Np oxide) and 254 (^{238}U oxide). Raw data were corrected for dead time of the electron multiplier and processed off-line in the Lamdate spreadsheet-based program (Košler et al. 2002). Data reduction included correction for the gas blank, laser-induced elemental fractionation of Pb and U and instrument mass bias. No common Pb correction was applied to the data. Calculation of mean ages and plotting of a Concordia diagram was performed with the Isoplot program of Ludwig (2003).

4. Petrology and P–T evolution of the Miřetín Pluton

The Miřetín Pluton is composed of two texturally different varieties of calc-alkaline granitoids: (i) coarse- to medium-grained biotite granodiorite and (ii) porphyritic amphibole–biotite granodiorite to tonalite with abundant microgranular enclaves of diorites and gabbros. In both textural varieties of the granodiorites, plagioclase grains have subhedral shapes and reveal oscillatory zoning well visible in optical CL. The anorthite contents continuously decrease rimwards (from $An_{31–36}$ to $An_{2–20}$, Tab. 2). K-feldspar ($Ab_{2–7}$) occurs as subhedral crystals. Biotite has ^{IV}Al = 2.32–2.60 apfu and Fe/(Fe + Mg) = 0.59–0.47 (Fig. 2a; Tab. 3); subhedral to anhedral amphibole corresponds to magnesiohornblende (Mg/(Fe + Mg) = 0.50–0.60, Si = 6.9–7.3 apfu; Fig. 2b, Tab. 4). Anhedral quartz grains form aggregates in interstitial domains. Apatite, monazite, zircon and titanite are common accessory minerals in both textural varieties.

Tab. 3 Selected chemical compositions of biotite (wt. % and apfu)

Sample	LV13S	LV13S	LV13S	LV13S	LV13S	L23	L23	L23	404
SiO_2	35.43	35.46	35.67	35.51	35.41	36.91	36.68	36.70	36.60
TiO_2	2.17	2.36	2.36	2.51	2.65	2.15	1.89	1.54	3.02
Al_2O_3	17.89	18.75	18.17	18.90	18.89	15.68	15.90	15.84	15.41
FeO	20.68	20.39	20.41	19.41	19.84	19.80	20.76	20.96	21.41
MnO	0.35	0.33	0.23	0.25	0.32	0.38	0.43	0.38	–
MgO	9.15	8.69	9.22	9.16	8.78	11.13	10.40	10.97	9.47
Na_2O	0.07	0.13	0.12	0.17	0.10	0.07	0.07	0.12	–
K_2O	9.68	9.79	9.79	9.86	9.53	9.36	9.40	9.40	10.03
BaO	0.11	0.20	0.08	0.14	0.09	0.30	0.26	0.29	–
F	0.01	0.00	0.00	0.03	0.08	0.00	0.01	0.07	–
Cl	0.13	0.11	0.11	0.11	0.12	0.07	0.09	0.10	–
H_2O*	3.87	3.91	3.91	3.91	3.87	3.92	3.89	3.87	3.91
O=F,Cl	0.03	0.03	0.03	0.04	0.06	0.02	0.02	0.05	0.00
Total	99.58	100.09	100.06	99.95	99.68	99.76	99.80	100.21	99.86
(apfu)									
Si	5.438	5.404	5.434	5.393	5.395	5.623	5.614	5.600	5.615
^{IV}Al	2.562	2.596	2.566	2.607	2.605	2.377	2.386	2.400	2.385
^{VI}Al	0.675	0.772	0.695	0.777	0.787	0.439	0.482	0.449	0.401
Ti	0.251	0.270	0.270	0.287	0.303	0.246	0.217	0.176	0.348
Fe	2.655	2.599	2.600	2.466	2.528	2.523	2.657	2.675	2.747
Mn	0.045	0.043	0.030	0.032	0.042	0.048	0.056	0.049	–
Mg	2.094	1.974	2.094	2.074	1.993	2.527	2.373	2.496	2.166
Na	0.022	0.040	0.037	0.049	0.030	0.021	0.020	0.037	–
K	1.895	1.903	1.902	1.911	1.852	1.819	1.834	1.830	1.962
Ba	0.007	0.012	0.005	0.008	0.005	0.018	0.015	0.018	–
F	0.005	0.000	0.000	0.014	0.040	0.000	0.002	0.032	–
Cl	0.034	0.029	0.030	0.028	0.031	0.019	0.022	0.025	–
OH*	3.960	3.971	3.970	3.958	3.928	3.981	3.975	3.943	4.000
ΣCAT.	19.643	19.613	19.633	19.604	19.541	19.641	19.655	19.728	19.624

Amphibole-rich mafic microgranular enclaves contain subhedral plagioclase with patchily zoned anorthite-rich cores ($An_{49–82}$) and relative homogenous andesine rim ($An_{30–31}$) and anhedral quartz grains. Amphibole in enclaves corresponds to magnesiohornblende (Mg/(Fe + Mg) = 0.56–0.60, Si = 6.6–7.0 apfu; Fig. 2b) partially replaced by actinolite (Mg/(Fe + Mg) = 0.68–0.69, Si = 7.7–7.8 apfu). Biotite (Fig. 2a, ^{IV}Al = 2.32–2.37 apfu and Fe/(Fe + Mg) = 0.47–0.49) is the most abundant near the boundary with granodiorite. Common accessory minerals are apatite, monazite, zircon and ilmenite ± titanite.

Estimated P–T conditions of 653–681 °C and 0.29–0.43 GPa (Fig. 2c, Tab. 5) obtained from the amphibole–plagioclase thermometer (Holland and Blundy 1994) and Al-in-hornblende barometer (Anderson and Smith 1995) reflect the final stages of magma crystallization or the subsequent high-T subsolidus deformation of the Miřetín Pluton granitoids.

5. Structural pattern

The eastern flank of the Hlinsko Unit exhibits a relatively simple structural pattern. Relics of bedding or an early subhorizontal spaced cleavage were observed. These fabrics have been intensely folded into moderately to steeply ~WNW or ~ESE dipping planes, mostly parallel to the ~NNE–SSW trending axial cleavages and new low-T schistosity. The axes of these folds have a subhorizontal NNE–SSW or gently NNE plunging orientation (Fig. 3).

The overall structural pattern in the central and eastern parts of the Polička Unit is defined by regional metamorphic foliation (pervasive metamorphic schistosity or compositional banding) dipping moderately to steeply to the ~NE or SW (Fig. 3). These regional foliations are associated with well-developed stretching and/or mineral lineation gently plunging to ~NW and indicators of right-lateral transpressional kinematics (e.g. meso- to

Tab. 4 Selected chemical compositions of amphibole (wt. % and apfu)

Sample	L23	L23	L23	404
SiO_2	48.15	46.45	46.25	46.27
TiO_2	0.39	0.56	0.55	1.15
Al_2O_3	7.82	9.20	9.11	7.83
Cr_2O_3	0.01	0.02	0.02	0.00
$Fe_2O_3^{calc}$	0.89	1.62	1.70	2.23
FeO^{calc}	14.78	14.96	14.90	15.65
MnO	0.51	0.55	0.55	0.45
MgO	11.56	10.91	10.81	10.78
CaO	12.17	12.11	12.06	12.03
Na_2O	0.91	0.99	0.98	0.88
K_2O	0.57	0.85	0.78	0.92
H_2O	2.05	2.04	2.03	2.03
Cl	0.05	0.06	0.06	0.00
O=Cl	-0.01	-0.01	-0.01	0.00
TOTAL	99.86	100.31	99.78	100.21
(apfu)				
Si	7.097	6.867	6.872	6.889
^{IV}Al	0.903	1.133	1.128	1.111
ΣT	8.000	8.000	8.000	8.000
^{VI}Al	0.455	0.470	0.468	0.262
Ti	0.044	0.062	0.062	0.129
Fe^{3+}	0.098	0.181	0.191	0.249
Cr	0.001	0.002	0.002	0.000
Mg	2.541	2.404	2.394	2.393
Fe^{2+}	1.821	1.850	1.851	1.948
Mn	0.040	0.031	0.032	0.019
ΣC	5.000	5.000	5.000	5.000
Mn	0.024	0.039	0.037	0.038
Ca	1.922	1.917	1.920	1.919
Na	0.053	0.044	0.043	0.043
ΣB	2.000	2.000	2.000	2.000
Na	0.208	0.239	0.239	0.211
K	0.107	0.161	0.147	0.175
ΣA	0.315	0.400	0.386	0.385
Cl	0.012	0.015	0.014	0.000
ΣCAT.	15.315	15.400	15.386	15.385

micro-scale asymmetric folds, localized shear zones and recrystallized quartz and feldspathic aggregates in pressure shadows, as well as asymmetric deformation of porphyroblasts).

In the northwestern part of the Polička Unit, the NW–SE trending regional fabrics described above were refolded into the NNE–SSW direction (Fig. 4a). New foliation planes dip steeply to moderately to the WNW and bear ~NW to NNW-plunging stretching lineations with indicators of top-to-the-E (thrusting) kinematics. Contacts between the Miřetín Pluton and host Polička Unit are intrusive. Their orientation is mostly parallel to the second NNE–SSW trending metamorphic fabrics identified in the northwestern part of the Polička Unit. Contacts between the upper-crustal Hlinsko Unit and Miřetín Pluton were modified by NNE–SSW trending normal fault (Fig. 3). According to the criteria defined by Paterson et al. (1998) and Vernon (2000), two distinct solid-state fabrics were identified in the Miřetín Pluton (Figs 4b, 5a–b).

High-T solid-state fabrics with some relics of submagmatic flow are defined by the ductile deformation with accompanying recrystallization of feldspars, quartz and biotite aggregates. This high-T solid-state foliation dips under moderate angles to the W to NW and bears well-developed stretching lineation plunging to WNW to N (ductile elongation of quartzo–feldspathic and biotite aggregates). The asymmetry of the deformed and recrystallized mineral aggregates and folded leucogranite dikes indicates thrusting kinematics (Fig. 4b–c). This high-T solid-state deformation was in some places localized into narrow zones of mylonites (Fig. 4d).

Second, sharply superimposed fabrics have a character of discrete low-T spaced cleavage (Fig. 4b, 5b), marked by localized brittle–ductile to brittle deformation and rare recrystallization. This cleavage dips under a moderate to steep angle to the WNW and is associated with moderately NW plunging stretching lineation (striations) and indicators of W-side-down kinematics. These low-T solid-state fabrics occur only in a narrow zone (up to 0.5 km wide) along the western flank of the Pluton and are parallel to the fault-controlled boundary between the Miřetín Pluton and structurally overlying Hlinsko Unit.

Tab. 5 The petrologically studied samples of plutonic rocks, their mineral assemblages and estimated P–T conditions

Sample	Locality	Rock	Mineral assemblage	Amp–Pl*	Amp**
404	Pastvisko	tonalite	Pl + Qtz + Kfs + Bt + Amp	659–675	0.29–0.35
L23	Kutřín	granodiorite	Pl + Qtz + Kfs + Bt + Amp	653–681	0.32–0.43
LV13S	Kutřín	granodiorite	Pl + Qtz + Kfs + Bt	–	–

* amphibole–plagioclase thermometer (Holland and Blundy 1994)
** Al-in-hornblende barometer (Anderson and Smith 1995)

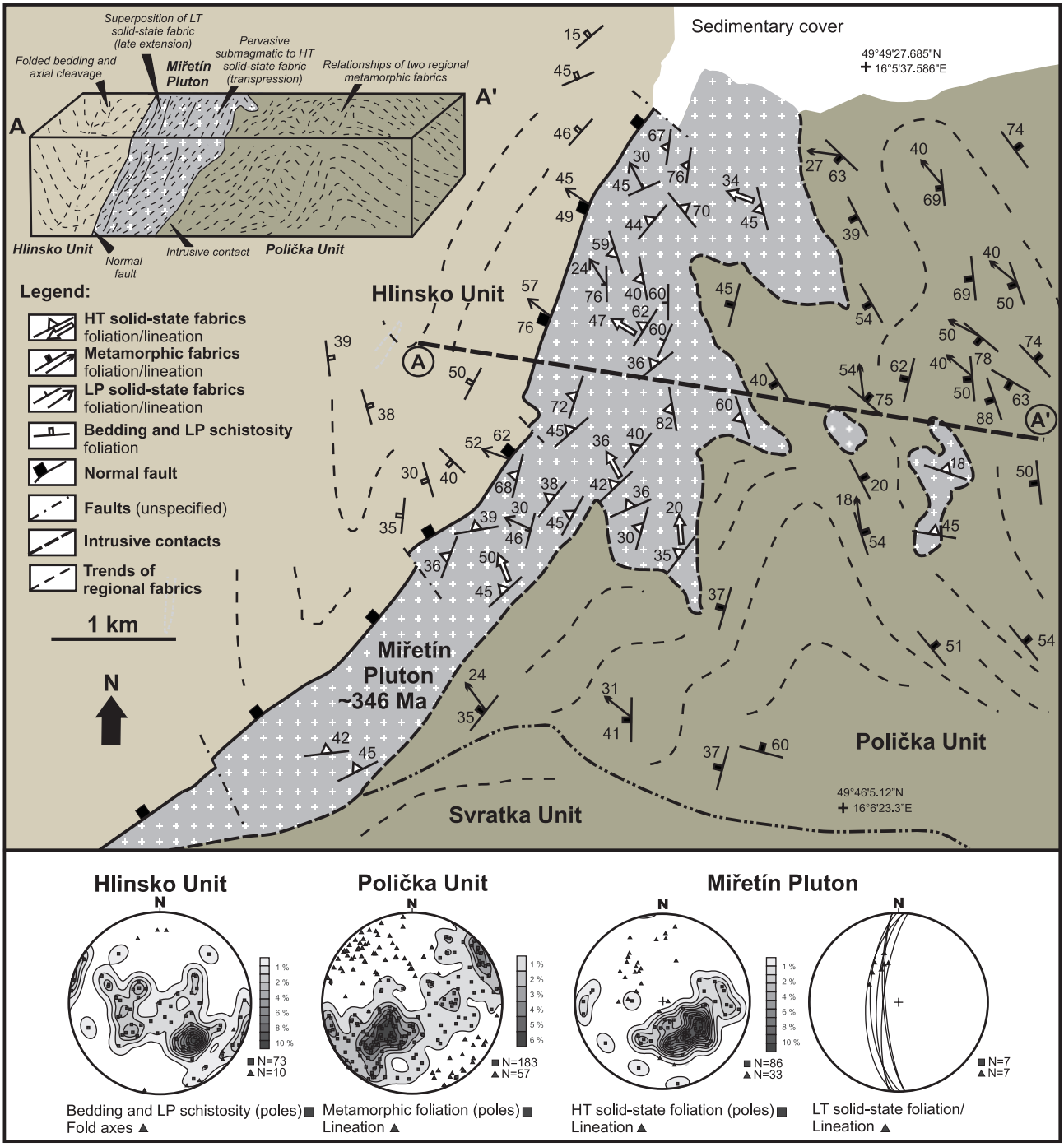

Fig. 3 Structural map of the Miřetín Pluton and its metamorphic host rocks of Polička and Hlinsko units. Below: orientation stereograms (lower hemisphere, equal area projection) of regional fabrics.

6. Microstructures and EBSD analyses

Microstructural analysis of Miřetín Pluton fabrics was carried out on the basis of 18 oriented thin-sections. According to the criteria of microstructural classification for deformed magmatic rocks (e.g. Paterson et al. 1989; Vernon 2000; Passchier and Trouw 2005), three distinct events of microstructural evolution were defined in the Miřetín Pluton: (i) fabrics of submagmatic flow which include an evidence for melt-supported intracrystalline deformation and recrystallization identified in relics; (ii) high-T solid-state fabrics involving features of penetrative crystal-plastic deformation and dynamic recrystallization (above ~500 °C); and (iii) low-T solid-state fab-

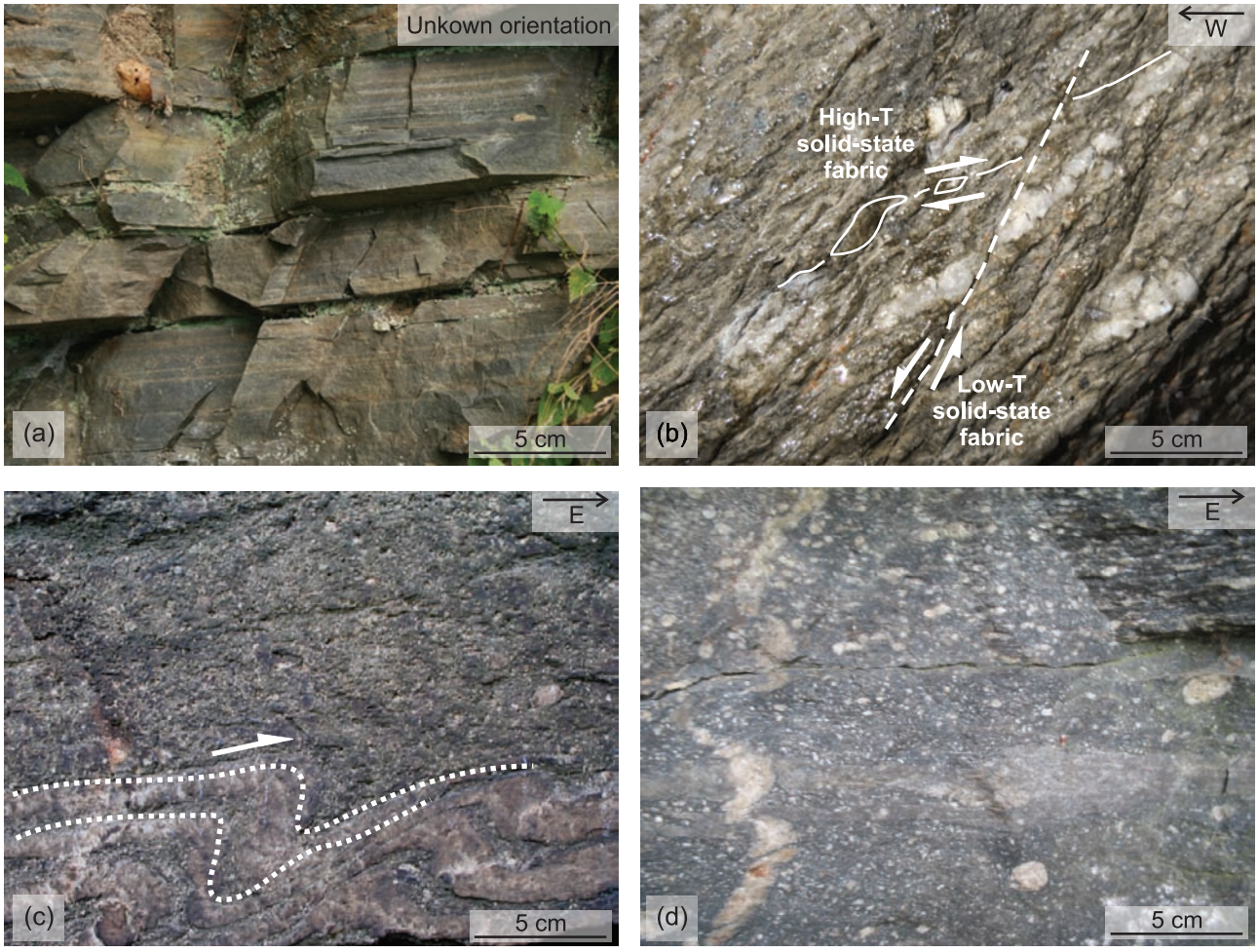

Fig. 4 Field photographs. **a –** Transpressional metamorphic foliation in paragneisses of the northwestern Polička Unit; **b** – Relationships between the high-T solid-state fabric with an evidence for thrusting kinematics and low-T solid-state fabrics bearing indicators of west-side-down kinematics (Miřetín Pluton); **c** – Asymmetrically folded leucogranite dikes in a zone of high-T solid-state deformation indicating thrusting kinematics (Miřetín Pluton); **d** – Mylonite zone with folded syntectonic dike of leucogranite composition (Miřetín Pluton).

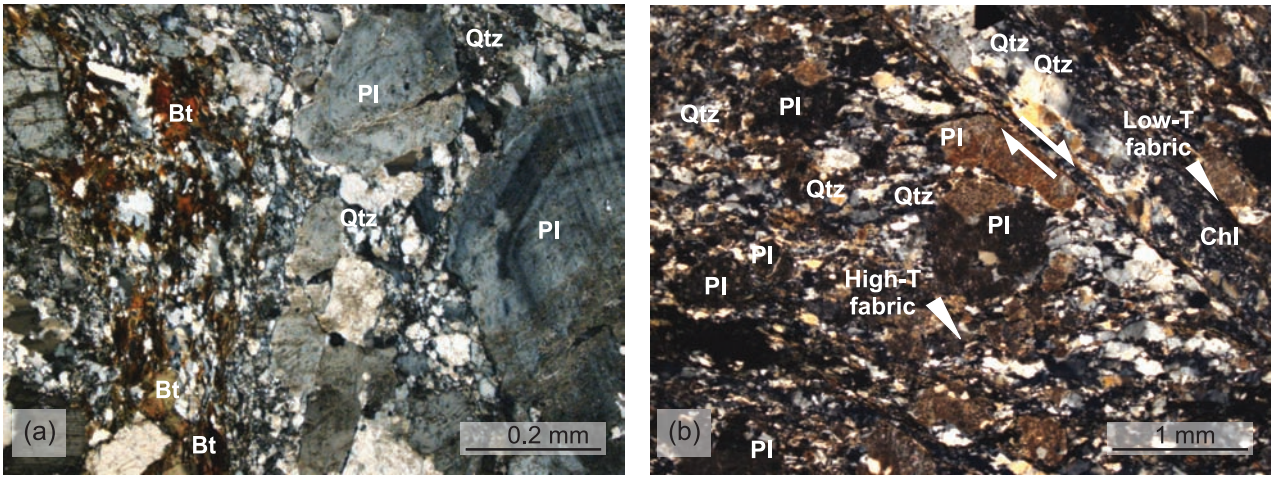

Fig. 5 Photomicrographs. **a** – Magmatic grains of plagioclase, K-feldspar, biotite and quartz affected by internal plastic deformation (recrystallization along grain boundaries and formation of deformation lamellae, i.e. "ribbon microstructure") bearing evidence for grain-boundary migration recrystallization; **b** – Microstructural evidence for superimposition of pervasive high-T solid-state fabrics and low-T solid-state deformation and recrystallization (cataclastic flow). Angular fragments of quartz and plagioclase grains as well as new chlorite aggregates occur in a very fine-grained matrix in discrete cleavage planes (western flank of the Miřetín Pluton).

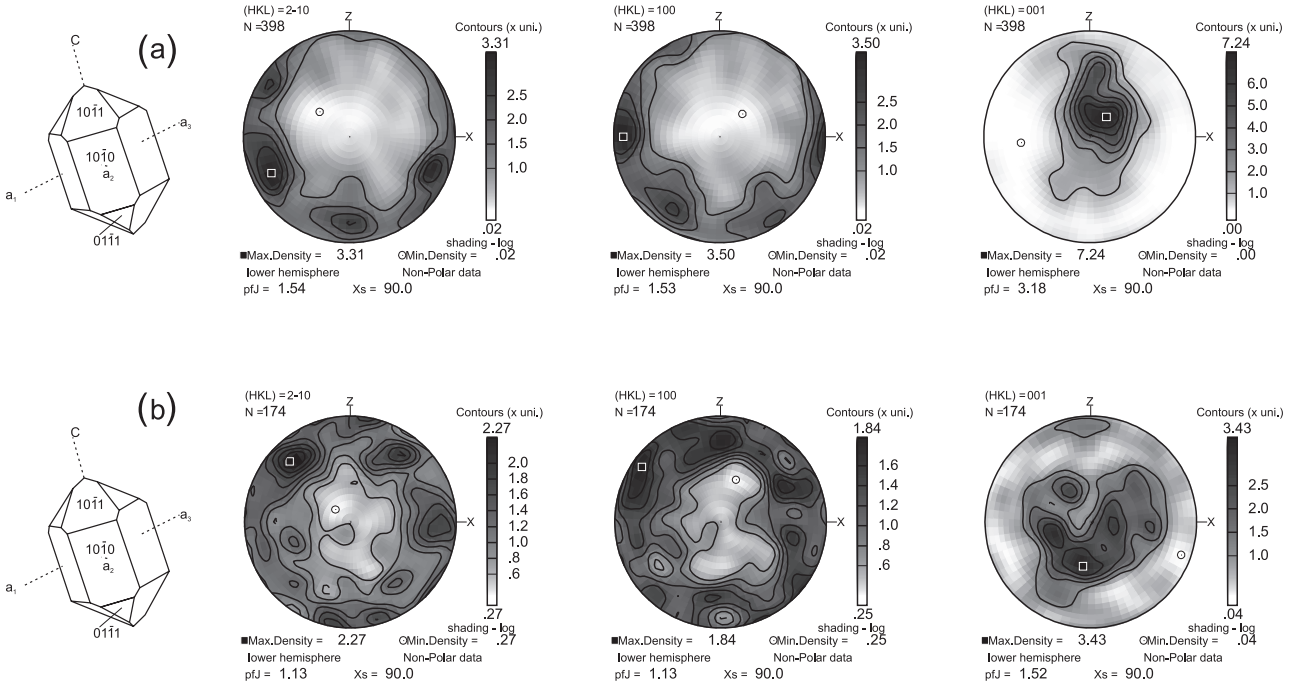

Fig. 6 Stereographic projection (equal area, lower hemisphere) of quartz *c* axes orientations obtained using the EBSD method shown in XZ section. The LPO patterns of high-T (**a**) and low-T (**b**) solid-state fabrics.

rics bearing evidence for superimposed non-penetrative and localized brittle–ductile to brittle deformation. Across the Miřetín Pluton, identified fabrics of submagmatic flow and high-T sub-solidus deformation vary in intensity and exhibit a transitional character.

6.1. Submagmatic flow

Evidence for submagmatic flow is preserved especially in the eastern part of the Miřetín Pluton, as the effects of penetrative high-T solid-state deformation continuously increase towards the west. The textures of the submagmatic stage include relics of magmatic preferred orientation of feldspars and amphiboles, evidence for crystallization of the melt remaining in interstitial domains and magmatic zoning in conjunction with a small amount of crystal-plastic deformation and recrystallization (Fig. 5a). The initial stages of crystal-plastic deformation and recrystallization (predominantly along fractures and crystal boundaries) were heterogeneous and focused into quartz and biotite aggregates. Quartz aggregates are slightly elongated and show undulose extinction, formation of a chessboard-pattern and interlobate shape of subgrains (0.1–0.4 mm in size). These microstructural features indicate activity of high-T grain boundary migration (GBM) recrystallization (Stipp et al. 2002). Some of biotite aggregates were affected by kinking and locally also by pressure dissolution. Feldspars were more resistant at this stage, bearing no evidence for internal crystal-plastic deformation. However, myrmekites and flame perthites can be locally observed.

6.2. High-T solid-state fabrics

Characteristic features of the high-T sub-solidus fabrics are as follows (Fig. 5a–b): (i) the presence of anastomosing foliation defined by folded and dynamically recrystallized biotite (with mica-fish texture) and quartz aggregates, both interconnected into narrow penetrative ribbons which commonly enclose less deformed porphyroblasts of feldspars; (ii) recrystallized aggregates of quartz and feldspar which reveal irregular and lobate shapes of new subgrains. The shape and degree of lattice preferred orientation of these sub-grains clearly indicate the high-T GBM recrystallization; (iii) the presence of mechanical twinning of feldspars, including formation of deformation lamellae, and (iv) abundant myrmekite and perthite textures.

6.3. Low-T solid-state fabrics

Effects of low-T sub-solidus deformation were identified locally in a relatively narrow zone along the western margin of the Pluton (Fig. 5b). Corresponding textures indicate brittle–ductile to brittle deformation. Quartz and feldspar aggregates are deformed by fracturing bearing a record of cataclastic flow (the presence of angular grain fragments in a very fine-grained matrix). Biotite

aggregates are occasionally fractured and recrystallized to chlorite subgrains (Fig. 5b).

6.4. Electron back-scatter diffraction (EBSD) analyses

Two samples were studied in order to evaluate the conditions of deformation. The first (LV136; Fig. 6a) exhibits high-T sub-solidus deformation without a subsequent brittle event. The measured quartz grains are anhedral, partly recrystallized. On a orientation diagram (Fig. 6a), the quartz *c* axes (001) show strong maxima near the centre. The *a* axes (100) produced two peaks on the periphery of diagram. According to Passchier and Trouw (2005), such a geometry probably corresponds to the prism <a> slip, which is active at moderate temperatures (*c.* 550 °C). The second sample (L90; Fig. 6b) showed small quartz grains, which were recrystallized in highly strained domains, reflecting the low-T subsolidus overprint. In this case, the EBSD results show maxima of *c* axes (001) in a relatively wide belt of N–S orientation. The *a* axes (100) define several peaks on the periphery of the stereonet. According to Passchier and Trouw (2005), such a geometry corresponds to the basal <a> slip, which is active at lower temperatures (*c.* 350 °C).

7. U–Pb dating of the Miřetín Pluton

Analysed zircon grains were separated from porphyritic amphibole–biotite granodiorite indicating clear evidence for transitional submagmatic to high-T deformation with no evidence for low-T recrystallization (sample L92; see Fig. 1c and Tab. 1 for its location). Zircon grains are euhedral, oscillatory zoned and prismatic with features pointing to crystallization from a granitoid magma. Rarely, some consist of oscillatory-zoned rims surrounding unzoned xenocrystic cores.

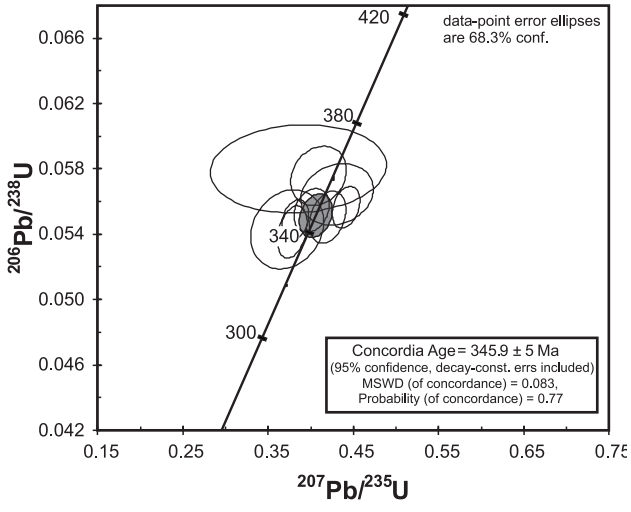

Fig. 7 U–Pb Concordia diagram for zircons of the Miřetín Pluton. The error ellipses are plotted with 1σ uncertainties.

The U–Pb data obtained by laser-ablation ICP-MS dating of fifteen zircon grains are given in Tab. 6 and plotted on Concordia diagram (Fig. 7). Zircon grains yielded concordant U–Pb ages with the mean of 345.9 ± 5 Ma (2σ), which is interpreted as the magmatic (crystallization) age.

8. Discussion

8.1. Age and genesis of the Miřetín Pluton

The granitoids of the Miřetín Pluton resemble geochemically other Variscan calc-alkaline intrusions that intruded marginal parts of the Teplá–Barrandian Zone (e. g. Holub 1997b; Janoušek et al. 2000, 2004; Buriánek et al. 2003). For this reason, the genesis of this Pluton was probably also associated with mixing of basic mantle-derived magmas from a suprasubduction environment with crustal melts of tonalite composition (Buriánek et al. 2003; Janoušek et al. 2004).

The newly determined U–Pb zircon age of the Miřetín Pluton (345.9 ± 5 Ma) differs somewhat from previously published geochronological data from the same (Schulmann et al. 2005). The relatively younger age of 327 ± 6 Ma established by the U–Pb zircon dissolution and vapour transfer method was similarly interpreted as timing the magma emplacement (Schulmann et al. 2005). Furthermore, the Pb–Pb evaporation age of 323 ± 1.1 Ma on the same sample was adopted as the time limit for the extensional shearing tectonics (Schulmann et al. 2005). The discrepancy of ~20 M.y. between our new and the previously published geochronological data may be caused by selection of different rock-samples, which could have been variously affected by high- to low-T deformation and recrystallization and use of different geochronological methods.

Our concordant age of 345.9 ± 5 Ma was obtained on sample taken from the least deformed domain of the Miřetín Pluton, which showed no evidence for low-T subsolidus overprint. This new result is consistent with reported ages for other calc-alkaline plutons of Variscan age emplaced into the rocks of the Teplá–Barrandian Unit (357–345 Ma; Holub et al. 1997a; Janoušek et al. 2004, 2010; Vondrovic and Verner 2010).

8.2. P–T conditions of regional metamorphism and magmatic crystallization

The metamorphic assemblage of cordierite hornfelses (Grt + Cdr + Bt + Ms + Pl ± And ± St) from the northwestern Polička Unit constrains the peak P–T conditions

Tab. 6 Results of U–Pb dating of the Miřetín Pluton (laser ablation ICP-MS)

Analysis	Concentrations		Atomic ratios						Apparent ages (Ma)					
	Pb	U	$^{207}Pb/^{235}U$	1σ	$^{206}Pb/^{238}U$	1σ	$^{207}Pb/^{206}Pb$	1σ	$^{207}Pb/^{235}U$	1σ	$^{206}Pb/^{238}U$	1σ	$^{207}Pb/^{206}Pb$	1σ
	µg/g	µg/g		(abs)		(abs)		(abs)		(abs)		(abs)		(abs)
070709JMa10	6	89	0.4185	0.0139	0.0551	0.0010	0.0541	0.0012	323.5	0.0139	328.7	0.001	376.9	51.5
070709JMa16	6	100	0.4299	0.0280	0.0564	0.0012	0.0554	0.0029	330.3	0.0280	363.5	0.0012	429.9	115.3
070709JMa21	11	186	0.4401	0.0108	0.0557	0.0008	0.0568	0.0011	379.0	0.108	327.4	0.0008	484.9	43.8
070709JMa23	9	150	0.4080	0.0216	0.0576	0.0012	0.0520	0.0021	321.3	0.216	328.3	0.0012	284.0	91.0
070709JMa25	7	125	0.3805	0.0104	0.0549	0.0008	0.0503	0.0012	416.3	0.0104	351.9	0.011	208.6	54.2
070709JMa26	6	102	0.3772	0.0112	0.0542	0.0011	0.0507	0.0013	341.5	0.0689	348.1	0.0035	227.3	58.6
070710JMa07	9	157	0.5068	0.0689	0.0561	0.0035	0.0648	0.0052	320.6	0.0136	341.1	0.0009	766.2	167.9
070710JMa14	5	81	0.3999	0.0136	0.0555	0.0009	0.0517	0.0014	381.4	0.0281	346.5	0.0016	271.9	63.8
070710JMa17	4	58	0.3713	0.0281	0.0543	0.0016	0.0505	0.0027	344.3	0.0422	329.4	0.001	217.5	125.6
070710JMa18	8	136	0.4559	0.0422	0.0552	0.0010	0.0631	0.0044	355.0	0.0239	345.6	0.0029	712.2	147.5
070710JMa21	8	139	0.4036	0.0239	0.0524	0.0029	0.0587	0.0044	363.1	0.0354	354.0	0.0019	556.9	163.8
070710JMa30	4	71	0.3752	0.0354	0.0523	0.0019	0.0518	0.0031	370.3	0.0683	349.2	0.0018	275.5	137.9
070710JMa31	5	87	0.3844	0.0683	0.0580	0.0018	0.0484	0.0066	347.4	0.0272	360.9	0.0016	120.1	322.8
070710JMa33	4	67	0.4525	0.0272	0.0521	0.0016	0.0627	0.0030	327.4	0.0329	344.5	0.0027	698.4	101.2
070710JMa37	4	56	0.3722	0.0329	0.0523	0.0027	0.0531	0.0030	325.0	0.00045	340.0	0.0009	333.7	126.9

with rare evidence for contact metamorphism to 559 ± 65 °C and 0.3 ± 0.2 GPa (Buriánek 2009). These results are roughly consistent with the P–T data newly estimated for the Miřetín Pluton (T = 653–681 °C and P = 0.29–0.43 GPa; Fig. 2c, Tab. 5) which could reflect the conditions of magma crystallization or closely following high-T recrystallization. Based on concordance of these P–T data, the Miřetín Pluton was clearly emplaced during the peak regional metamorphism of the host Polička Unit. On the other hand, metapelites from the Hlinsko Unit reflect cooling from ~600 °C to 530 °C and a slight increase in pressure from *c.* 0.36 GPa to 0.40 GPa (Pitra and Guiraud 1996). The lithological compositions as well as estimated P–T conditions from the Hlinsko and Polička units suggest that these rocks had a similar protolith and were affected by comparable P–T path of the Variscan regional metamorphism. Subtle differences in P–T conditions and structural pattern can be explained by the later NNW–SSE normal faulting between the Polička Unit and the overlying Hlinsko Unit.

8.3. Fabrics and emplacement of the Miřetín Pluton

The ~346 Ma Miřetín Pluton was emplaced into the upper- to mid-crustal rocks of the Polička Unit and probably also into the Hlinsko Unit (at a depth of *c.* 10 km), which were synchronously affected by two distinct stages of transpressional (compressional) deformation (Verner et al. 2009; Pertoldová et al. 2010). Intrusive contacts and internal fabrics of the Miřetín Pluton dip at moderate angles to ~WNW (Fig. 3) and thus are oriented at a high angle to the regional transpressional fabrics well preserved in all units at the NE periphery of the Moldanubian Zone (Verner et al. 2009). Structures in the Miřetín Pluton are mostly parallel to the superimposed compressional fabrics in the northwestern Polička Unit. In addition, microstructural and EBSD analyses of the Miřetín Pluton reveal two distinct sub-solidus fabrics: (i) contact subparallel, pervasive transitional submagmatic to high-T foliation (>500 °C) associated with well-developed stretching lineation bearing evidence for thrusting kinematics and (ii) low-T (~350 °C), sharply superimposed cleavage planes with an evidence for west-side-down kinematics identified in a narrow NNW–SSE zone along the western part of the Miřetín Pluton. This structural pattern (i.e. the presence of pervasive submagmatic to high-T solid-state fabrics and mostly parallel orientation of the intrusive contacts in relation to the regional metamorphic fabrics) resembles highly asymmetric sheet-like magmatic bodies syntectonically emplaced during regional transpressional (compressional) event (e.g. Brown and Solar 1999). The ascent and emplacement of the Miřetín Pluton into higher crustal levels caused presumably limited softening of the host rocks and synkinematic growth of LP–HT metamorphic assemblages. This thermal anomaly resulted in an increasing ductile deformation in and around the Pluton, with the same orientation as the superimposed metamorphic fabrics in the northwestern Polička Unit. In general, all these fabrics reflected the orientation of the regional strain field (the WNW–ESE shortening and perpendicular stretching). Our interpretation of the emplacement and geodynamic evolution of the Miřetín Pluton as well as the regional context of the host rocks discussed above is at variance with the earlier concepts of Pitra et al. (1994),

Pitra and Guiraud (1996) and Schulmann et al. (2005) who interpreted the Miřetín Pluton as a synkinematic laccolith within a shallow-dipping normal shear zone between the Hlinsko metasedimentary sequence and high-grade rocks of the Svratka Unit at around 327 Ma.

8.4. Regional tectonic evolution

Age, emplacement and subsequent solid-state deformation of the Miřetín Pluton point to synmagmatic activity of the NNE–SSW trending transpression zone, which also affected the upper- to mid-crustal units outside the E margin of the Teplá–Barrandian Zone (e.g. Žák et al. 2005, 2009). This agrees well with interpretation of the transition from transpression to large-scale exhumation of the Variscan orogenic root along the Teplá Barrandian/Moldanubian boundary dated at 346 Ma (Žák et al. 2005; Janoušek et al. 2010). Sharply superimposed low-T cleavages are consistent with the NNW–SSE trending normal fault zone located between the Polička Unit and the overlying Hlinsko Unit. On a regional scale, their origin was associated with a ~WNW–ESE extensional event assumed to have occurred after 335 Ma (Verner et al. 2006; Pertoldová et al. 2010).

9. Conclusions

The Miřetín Pluton (dated at 345.9 ± 5 Ma; U–Pb on zircons) belongs to the group of calc-alkaline intrusions emplaced into marginal parts of the eastern Teplá–Barrandian Zone. The Miřetín Pluton intruded the units rimming the northern margin of the high-grade Moldanubian Zone. Its emplacement into the upper- to mid-crustal levels of the Variscan continental crust took place during, or shortly after, their peak metamorphism (at *c.*10 km). Magma was intruded syntectonically into a NNE–SSW oriented transpressional domain, whereby the shortest dimension of the Miřetín Pluton was roughly parallel to the direction of principal shortening. During, or closely after, its emplacement, the Pluton was affected by pervasive submagmatic to high-T solid-state deformation, reflecting the last increment of regional strain-field of this NNE–SSW trending transpressional zone at *c.* 580 °C and 0.4 GPa. The NNE–SSW oriented boundary between the Miřetín Pluton and the structurally overlying Hlinsko Unit bears microstructural evidence of low-T normal faulting, which originated during a regional extensional event, probably later than 335 Ma.

Acknowledgements. Thorough reviews by Eckardt Stein and Carlo Dietl improved greatly this manuscript and are gratefully acknowledged. We would also like to thank František V. Holub for helpful discussion and we appreciate the assistance of Renata Čopjaková at the electron microprobe. We also thank Jiří Žák and Vojtěch Janoušek for careful editorial work. This research was supported by the Grant Agency of Charles University research project No. 81909, the Ministry of Education, Youth and Sports of the Czech Republic through Research Plan No. MSM0021620855, the Czech Geological Survey research project No. 323000 and Grant Agency of Czech Republic project No. 205/09/0630.

References

Anderson JL, Smith DR (1995) The effects of temperature and fO_2 on the Al-in-hornblende barometer. Amer Miner 80: 549–559

Bonlen SR, Peacor DR, Essene EJ (1980) Crystal chemistry of a metamorphic biotite and its significance in water barometry. Amer Miner 65: 55–62

Brown M, Solar GS (1999) The mechanism of ascent and emplacement of granite magma during transpression: a syntectonic granite paradigm. Tectonophysics 312: 1–33

Buriánek D (2009) Petrography of the Polička crystalline Complex. Acta Mus Moraviae Sci Nat 94: 3–46 (in Czech)

Buriánek D, Pertoldová J (2009) Garnet-forming reactions in calc-silicate rocks from the Polička Unit, Svratka Unit and SE part of the Moldanubian Zone. J Geosci 54: 245–268

Buriánek D, Němečková M, Hanžl P (2003) Petrology and geochemistry of plutonic rocks from the Polička and Zábřeh crystalline units (NE Bohemian Massif). Bull Czech Geol Surv 78: 9–22

Cháb J, Suchý V, Vejnar Z (1995) Moldanubian region; Teplá–Barrandian Zone (Bohemicum) – Metamorphic evolution (Chapter VII.B4). In: Dallmeyer RD, Franke W, Weber K (eds) Pre-Permian Geology of Central and Eastern Europe. Springer-Verlag, Berlin, 403–410

Cháb J, Breiter K, Fatka O, Hladil J, Kalvoda J, Šimůnek Z, Štorch P, Vašíček Z, Zajíc J, Zapletal J (2010) Outline of the Geology of the Bohemian Massif: the Basement Rocks and their Carboniferous and Permian Cover. Czech Geological Survey, Prague, pp 1–296

Chardon D, Andronicos CL, Hollister LS (1999) Large-scale transpressive shear zone patterns and displacements within magmatic arcs: the Coast Plutonic Complex, British Columbia. Tectonics 18: 278–292

Dunstan LP, Gramlich JW, Barnes IL, Purdy WC (1980) Absolute isotopic abundance and the atomic weight of a reference sample of thallium. J Res Nat Bur Stand 85: 1–10

Finger F, Roberts MP, Haunschmid B, Schermaier A, Steyrer HP (1997) Variscan granitoids of central Europe: their typology, potential sources and tectonothermal relations. Mineral Petrol 61: 67–96

Franke W (2000) The mid-European segment of the Variscides: tectonostratigraphic units, terrane boundaries and plate tectonic evolution. In: Franke W, Haak W, Oncken O, Tanner D (eds) Orogenic Processes: Quantification and Modelling in the Variscan Belt. Geological Society of London Special Publications 179: 35–63

Holland T, Blundy J (1994) Non-ideal interactions in calcic amphiboles and their bearing on amphibole–plagioclase thermometry. Contrib Mineral Petrol 116: 433–447

Holub FV, Cocherie A, Rossi P (1997a) Radiometric dating of granitic rocks from the Central Bohemian Plutonic Complex (Czech Republic): constraints on the chronology of the thermal and tectonic events along the Moldanubian–Barrandian boundary. C R Acad Sci Paris Earth Planet Sci 325: 19–26

Holub FV, Machart J, Manová M (1997b) The Central Bohemian Plutonic Complex: geology, chemical composition and genetic interpretation. Sbor geol Věd, Ložisk Geol Mineral 31: 27–50

Horn I, Rudnick RL, McDonough WF (2000) Precise elemental and isotope ratio determination by simultaneous solution nebulization and laser ablation ICP-MS: application to U–Pb geochronology. Chem Geol 164: 281–301

Hrouda F, Táborská Š, Schulmann K, Ježek J, Dolejš D (1999) Magnetic fabric and rheology of co-mingled magmas in the Nasavrky Plutonic Complex (E. Bohemia): implications for intrusive strain regime and emplacement mechanism. Tectonophysics 307: 93–111

Janoušek V, Bowes DR, Rogers G, Farrow CM, Jelínek E (2000) Modelling diverse processes in the petrogenesis of a composite batholith: the Central Bohemian Pluton, Central European Hercynides. J Petrol 41: 511–543

Janoušek V, Braithwaite C, Bowes DR, Gerdes A (2004) Magma-mixing in the genesis of Hercynian calc-alkaline granitoids: an integrated petrographic and geochemical study of the Sázava intrusion, Central Bohemian Pluton, Czech Republic. Lithos 78: 67–99

Janoušek V, Wiegand B, Žák J (2010) Dating the onset of Variscan crustal exhumation in the core of the Bohemian Massif: new U–Pb single zircon ages from the high-K calc-alkaline granodiorites of the Blatná suite, Central Bohemian Plutonic Complex. J Geol Soc, London 167: 347–360

Košler J, Sylvester PJ (2003) Present trends and the future of zircon in geochronology: laser ablation ICP-MS. In: Hanchar JM, Hoskin PWO (eds) Zircon. Mineralogical Society of America Reviews in Mineralogy and Geochemistry 53: 243–275

Košler J, Fonneland H, Sylvester P, Tubrett M, Pedersen RB (2002) U–Pb dating of detrital zircons for sediment provenance studies – a comparison of laser ablation ICP-MS and SIMS techniques. Chem Geol 182: 605–618

Kretz R (1983) Symbols for rock-forming minerals. Amer Miner 68: 277–279

Leake BE, Woolley AR, Arps CES, Birch WD, Gilbert MC, Grice JD, Hawthorne FC, Kato A, Kisch HJ, Krivovichev VG, Linthout K, Laird J, Mandarino J, Maresch WV, Nickel EH, Rock NMS, Schumacher JC, Smith DC, Stephenson NCN, Ungaretti L, Whittaker EJW, Youzhi G (1997) Nomenclature of amphiboles. Report of the Subcommittee on Amphiboles of the International Mineralogical Association Commission on New Minerals and Mineral Names. Eur J Mineral 9: 623–651

Ludwig KR (2003) Isoplot/Ex version 3.00. A Geochronological Toolkit for Microsoft Excel, User's Manual. Berkeley Geochronology Center Special Publications 4: 1–70

Miller RB, Paterson SR (2001) Construction of mid-crustal sheeted plutons: examples from the North Cascades, Washington. Geol Soc Am Bull 113: 1423–1442

Mísař Z, Dudek A, Havlena V, Weiss J (1983) Geology of the Bohemian Massif. SPN, Prague, pp 1–334 (in Czech)

Passchier CW, Trouw RAJ (2005) Microtectonics. Springer-Verlag, Berlin, pp 1–366

Paterson SR, Vernon RH, Tobisch OT (1989) A review of criteria for identification of magmatic and tectonic foliations in granitoids. J Struct Geol 11: 349–363

Paterson SR, Fowler TK, Schmidt KL, Yoshinobu AS, Yuan ES, Miller RB (1998) Interpreting magmatic fabric patterns in plutons. Lithos 44: 53–82

Pertoldová J, Verner K, Vrána S, Buriánek D, Štědrá V, Vondrovic L (2010) Comparison of lithology and tectonometamorphic evolution of units at northern margin of the Moldanubian Zone: implications for geodynamic evolution in the northeastern part of the Bohemian Massif. J Geosci 55: 299–319

Pitra P, Guiraud M (1996) Probable anticlockwise P–T evolution in extending crust: Hlinsko region, Bohemian Massif. J Metamorph Geol 14: 49–60

Pitra P, Burg JP, Schulmann K, Ledru P (1994) Late-orogenic extension in the Bohemian Massif: petrostructural evidence in the Hlinsko region. Geodin Acta 6: 15–31

Prior DJ, Boyle AP, Brenker F, Cheadle MC, Day A, Lopez G, Peruzzo L, Potis GJ, Reddy S, Spiess R, Timms NE, Trimby P, Wheeler J, Zettrstrom L (1999) The application of electron backscatter diffraction and orientation contrast imaging in the SEM to textural problems in rocks. Amer Miner 84: 1741–1759

Saint Blanquat M, Tikoff B, Teyssier Ch, Vigneresse JL (1998) Transpressional kinematics and magmatic arcs. In: Holdsworth RE, Strachan RA, Dewey JE (eds) Continental Transpressional and Transtensional Tectonics. Geological Society of London Special Publications 135: 327–340

Schmidt NH, Olensen NO (1989) Computer-aided determination of crystal-lattice orientation from electron-channelling patterns in the SEM. Canad Mineral 28: 15–22

Schmidt KL, Paterson SR (2002) A doubly vergent fan structure in the Peninsular Ranges Batholith: transpression or local complex flow around a continental margin buttress? Tectonics 21: 1050–1069

Schulmann K, Kröner A, Hegner E, Wendt I, Konopásek J, Lexa O, Štípská P (2005) Chronological constraints on the pre-orogenic history, burial and exhumation of deep-seated rocks along the eastern margin of the Variscan Orogen, Bohemian Massif, Czech Republic. Amer J Sci 305: 407–448

Schulmann K, Lexa O, Štípská P, Racek M, Tajčmanová L, Konopásek J, Edel JB, Peschler A, Lehmann J (2008) Vertical extrusion and horizontal channel flow of orogenic lower crust: key exhumation mechanisms in large hot orogens? J Metam Geol 26: 273–297

Schulmann K, Konopásek J, Janoušek V, Lexa O, Lardeaux JM, Edel JB, Štípská P, Ulrich S (2009) An Andean type Palaeozoic convergence in the Bohemian Massif. C R Geosci 341: 266–286

Stárková I ed. (1998) Basic geological map 1:50 000, sheet 14–33 Polička. Czech Geological Survey, Prague

Stipp M, Stuenitz Stünitz H, Heilbronner R, Schmid SM (2002) Dynamic recrystallization of quartz; correlation between natural and experimental conditions. In: Meer DS, Drury MR, Bresses JHP, Pennock GM (eds) Deformation Mechanisms, Rheology and tectonics; Current Status and Future Perspectives. Geological Society of London Special Publications 200: 171–190

Štorch P, Kraft P (2009) Graptolite assemblages and stratigraphy of the Lower Silurian Mrákotín Formation, Hlinsko Zone, NE interior of the Bohemian Massif (Czech Republic). Bull Geosci 84: 51–74

Tikoff B, Greene D (1997) Stretching lineations in transpressional shear zones: an example from the Sierra Nevada Batholith, California. J Struct Geol 19: 29–39

Vachtl J (1962) The Hlinsko Palaeozoic and its relationship to neighbouring units. Sbor Ústř Úst geol 27: 341–359 (in Czech)

Verner K, Žák J, Hrouda F, Holub FV (2006) Magma emplacement during exhumation of the lower- to mid-crustal orogenic root; the Jihlava syenitoid pluton, Moldanubian Unit, Bohemian Massif. J Struct Geol 28: 1553–1567

Verner K, Žák J, Nahodilová R, Holub FV (2008) Magmatic fabrics and emplacement of the cone-sheet-bearing Knížecí Stolec durbachitic Pluton (Moldanubian Unit, Bohemian Massif): implications for mid-crustal reworking of granulitic lower crust in the Central European Variscides. Int J Earth Sci 97: 19–33

Verner K, Buriánek D, Vrána S, Vondrovic L, Pertoldová J, Hanžl P, Nahodilová R (2009) Lithological and structural features of geological units along the northern periphery of the Moldanubian Zone: a review of the geology of the northeastern Variscides. J Geosci 54: 87–100

Vernon RH (2000) Review of microstructural evidence of magmatic and solid-state flow. El Geosci 5: 2, 1–23, doi: 10.1007/s10069-000-0002-3

Vondrovic L, Verner K (2010): The record of structural evolution and U–Pb zircon dating of the tonalite intrusions (Polička Crystalline Unit, Bohemian Massif). Trab Geol 30: 316–321

Vrána S, Blümel P, Petrakakis K (1995) Moldanubian Zone – Metamorphic Evolution (Chapter VII.C.4). In: Dallmeyer RD, Franke W, Weber K (eds) Pre-Permian Geology of Central and Eastern Europe. Springer-Verlag, Berlin, pp 453–468

Würm A (1927) The age of cherts in Hlinsko area. Věst St geol Úst Čs Republ 3: 247–255 (in Czech)

Žák J, Schulmann K, Hrouda F (2005) Multiple magmatic fabrics in the Sázava Pluton (Bohemian Massif, Czech Republic): a result of superposition of wrench-dominated regional transpression on final emplacement. J Struct Geol 27: 805–822

Žák J, Dragoun F, Verner K, Chlupáčová M, Holub FV, Kachlík V (2009) Forearc deformation and strain partitioning during growth of a magmatic arc: the northwestern margin of the central Bohemian Plutonic Complex. Tectonophysics 469: 93–111

Žák J, Kratinová Z, Trubač J, Janoušek V, Sláma J, Mrlina J (2011) Structure, emplacement, and tectonic setting of Late Devonian granitoid plutons in the Teplá–Barrandian Unit, Bohemian Massif. Int J Earth Sci 100: 1477–1495